Kinetic, Raman, NMR, and Site-Directed Mutagenesis Studies of the *Pseudomonas* Sp. Strain CBS3 4-Hydroxybenzoyl-CoA Thioesterase Active Site†

Zhihao Zhuang, Feng Song, Wenhai Zhang,‡ Kimberly Taylor,‡ Angela Archambault, and Debra Dunaway-Mariano*

Department of Chemistry, University of New Mexico, Albuquerque, New Mexico 87131

Jian Dong and Paul R. Carey*

Department of Biochemistry, Case Western Reserve University, Cleveland, Ohio 44106

Received June 3, 2002; Revised Manuscript Received July 15, 2002

ABSTRACT: 4-Hydroxybenzoyl-coenzyme A (4-HBA-CoA) thioesterase catalyzes the hydrolysis of 4-HBA-CoA to 4-hydroxybenzoate and CoA. X-ray crystallographic analysis of the liganded enzyme has shown that the benzoyl thioester and pantetheine moieties of the substrate ligand are bound in a narrow crevice while the nucleotide moiety rests on the protein surface (Thoden, J. B., Holden, H. M., Zhuang, Z. and Dunaway-Mariano, D. (2002) X-ray Crystallographic Analyses of Inhibitor and Substrate Complexes of Wild-type and Mutant 4-Hydroxybenzoyl-CoA Thioesterase, *J. Biol. Chem.*, in press). Asp17 is positioned in the crevice, close to the substrate thioester C═O, which in turn interacts with the positive pole of an α-helix macrodipole. In this paper we report the results from spectral, mutagenesis, and kinetic studies which show (1) that substrate activation involves restricted thioester C═O conformational freedom and a modest enhancement of C═O bond polarization, (2) that the nucleotide unit of the substrate is bound through interaction with the protein surface, and (3) that Asp17 contributes a rate factor of 10^4, consistent with its proposed role of general base or nucleophile.

Acyl-CoA thioesterases participate in a wide range of cellular processes; yet few thioesterase structures have been reported, and little is known about their catalytic mechanisms (*1*−*10*). In this paper we examine for the first time the mechanism of substrate recognition and catalysis by a member of the "hotdog-fold" family of thioesterases. The hotdog fold is a long α-helix cradled by a 7-stranded antiparallel *β*-sheet (*11*). This fold has been observed in the X-ray crystal structures of *Pseudomonas* sp. strain CBS-3 4-hydroxybenzoyl-coenzyme A (4-HBA-CoA) thioesterase (*1*), the focus of this work, *E. coli β*-hydroxydecanoyl-ACP desaturase (*11*), after which the hotdog fold was named, and *E. coli* long-chain acyl-CoA thioesterase II (*2*), which is comprised of two hotdog-fold domains connected by a linker region. Each of these enzymes recognizes a pantethiene-linked acyl-thioester as substrate: acyl-CoA in the cases of the two thioesterases and acyl-acyl carrier protein in the case of the desaturase.

4-HBA-CoA thioesterase catalyzes the hydrolysis of 4-HBA-CoA to 4-hydroxybenzoate (4-HBA) and CoA, the final step of the 4-chlorobenzoate degradation pathway (Scheme 1) found in certain soil-dwelling bacteria (*12*). 4-HBA is processed through aromatic oxidation pathways which ultimately feed the citric acid cycle. The 4-HBA-CoA thioesterase liberates 4-HBA for energy metabolism and CoA for participation in other cellular reactions.

In a recent paper, we reported three X-ray crystal structures of *Pseudomonas* sp. strain CBS3 4-HBA-CoA thioesterase (*13*). Two of these were of the wild-type thioesterase complexed to the inhibitor 4-hydroxyphenacyl-CoA (in this substrate analogue, the O═C−SCoA is replaced with O═C−CH_2−SCoA; see Chart 1) or to the inhibitor 4-hydroxybenzyl-CoA (the thioester C═O is replaced with CH_2). The third structure was of the catalytically impaired D17N mutant bound with the substrate 4-HBA-CoA. These structures presented a consistent picture of enzyme−substrate interactions.

As illustrated in Figure 1, the thioesterase is a dimer of dimers. There are two ligand binding sites per dimer, each located at the subunit interface. The benzoyl thioester and pantetheine moieties of the ligand are bound in a narrow crevice while the nucleotide moiety rests on the protein

† This work was supported by NIH Grant GM28688 to D.D.-M. and NIH Grant GM-54072 to P.R.C.

* To whom correspondence should be addressed. D.D.-M.: tel 505-277-3383, fax 505-277-6202, e-mail dd39@unm.edu. P.R.C.: tel 216-368-0031, fax 216-368-3419, e-mail carey@biochemistry.cwru.edu.

‡ Current address of W.Z. is Smith-Kline-Glaxo-Beecham and of K.L.T. is Nabi 12276, Wilkins Ave, Rockville, MD20852.

[1] Abbreviations used are: 4-HBA, 4-hydroxybenzoate; CoA, coenzyme A; 4-HBA-CoA, 4-hydroxybenzoyl-coenzyme A; 4-HP-CoA, 4-hydroxyphenacyl-coenzyme A; 4-HB-CoA, 4-hydroxybenzyl-coenzyme A; NADPH, dihydronictotinamide adenine dinucleotide phosphate; FAD, flavin adenine dinucleotide; PCR, polymerase chain reaction; NMR, nuclear magnetic resonance; Tris, tris-(hydroxymethyl)-aminomethane; K^+Hepes, potassium salt of N-(2-hydroxyethyl)piperzine-N′-2-ethanesulfonic acid; SDS-PAGE, sodium dodecylsulfate-polyacrylamide gel electrophoresis; H-bond, hydrogen bond.

10.1021/bi0262303 CCC: $22.00 © 2002 American Chemical Society
Published on Web 08/22/2002

Scheme 1: 4-Chlorobenzoate Dehalogenation Pathway

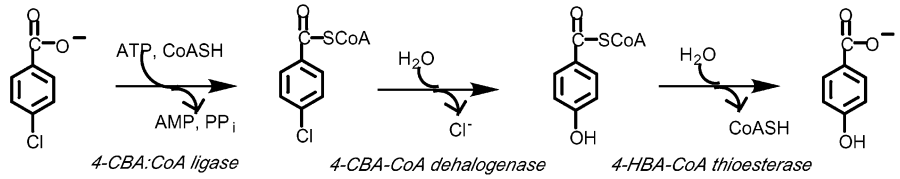

Chart 1

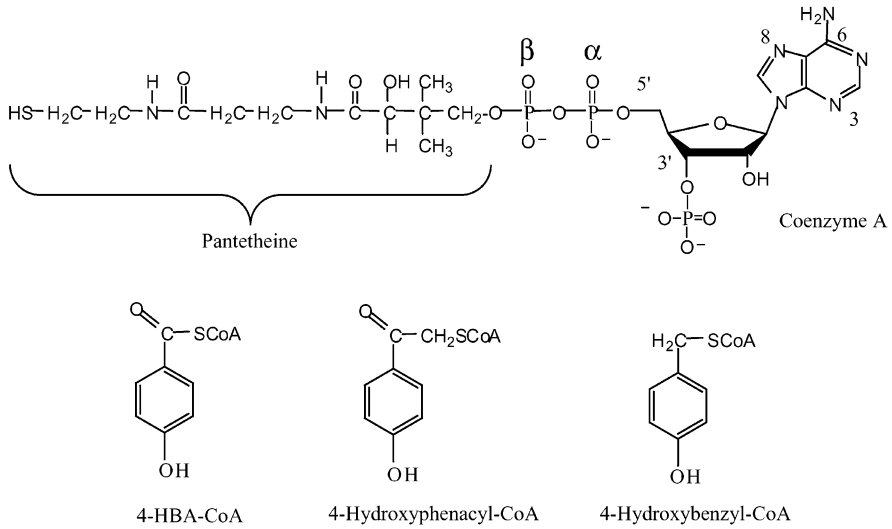

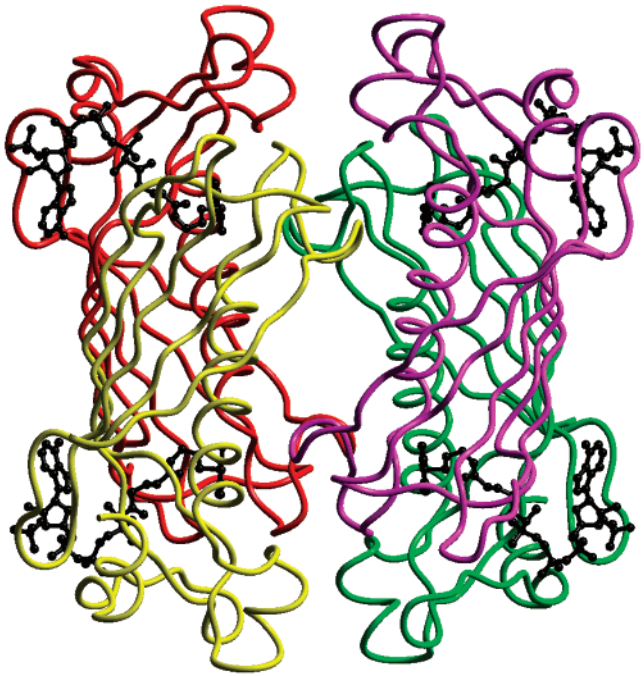

FIGURE 1: Structure of the *Pseudomonas* sp. strain CBS3 4-HBA-CoA thioesterase D17N mutant tetramer in which the four subunits are individually colored and the 4-HBA-CoA ligands are black. The figure was generated using Insight II and the X-ray coordinates of the D17N 4-HBA-CoA thioesterase−4-HBA-CoA complex (*13*).

surface. Asp17 is positioned in the crevice, close to the substrate thioester C═O, which in turn interacts with the positive pole of an α-helix macrodipole.

The structures of the liganded thioesterase raised several questions regarding substrate recognition and catalysis: (1) does the CoA moiety contribute to substrate binding? (2) what role does Asp17 play in catalysis? and (3) does the active site polarize the thioester C═O? In this paper we report the results from spectral, mutagenesis, and kinetic studies that were carried out to determine the answers to these questions.

MATERIALS AND METHODS

Materials. Wild-type *Pseudomonas* sp. strain CBS3 4-HBA-CoA thioesterase was prepared from the *E. coli* clone as described in ref *14*. 4-Hydroxyphenacyl-CoA, 4-HBA-(3′-dephospho)CoA, 4-HBA-CoA, and 4-HBA-pantetheine were prepared according to published procedures (*15*). Mutagenesis was carried out using a PCR strategy (*16*) based on the wild-type thioesterase gene (*14*) as template, commercial primers, the PCR kit supplied by Stratagene, and the Power Block IITM System thermal cycler manufactured by ERI-COMP. PCR-amplified DNAs were cloned into pET-3a vector (Novagen) for expression in *E. coli* HMS174 (DE3). The mutated genes were verified by DNA sequencing. The mutant proteins were purified by the same procedure used for the wild-type thioesterase and shown to be homogeneous by SDS−PAGE gel analysis. The yields of the pure proteins in mg/g wet cells were as follows: wild-type (10), D17E (8), D17N (5), D17S (5), R88A (8), R89L (5), K90A (3), R126L (10), and R128A (10).

Kinetic and Thermodynamic Constants. k_{cat}, K_m, and K_i Determinations. The initial velocity of the 4-HBA-CoA thioesterase catalyzed hydrolysis of 4-HBA-CoA was measured using the 4-HBA hydroxylase coupled spectrophotometric assay described in ref *14*. Reactions were carried out in 50 mM K$^+$Hepes (pH 7.5, 25 °C) containing wild-type or mutant 4-HBA-CoA thioesterase, 0.1 mM NADPH, 0.1 mM FAD, 0.5 unit/ml 4-HBA hydroxylase, and varying concentrations of 4-HBA-CoA ($0.5-10\times K_m$) with ($2\times K_i$) or without 4-hydroxyphenacyl-CoA inhibitor (linear inhibi-

tion was first tested). For all measurements, the initial velocity data were analyzed using eqs (1) or (2) and the computer program KinetAsyst (IntelliKinetics, PA): where

$$V = V_{max}\,[S]/([S] + K_m) \quad (1)$$

$$V = V_{max}\,[S]/[K_m\,(1+[I]/K_i) + [S]] \quad (2)$$

V = initial velocity, V_{max} = maximum velocity, [S] = substrate concentration, K_m = Michaelis constant, [I] = inhibitor concentration, and K_i = the inhibition constant. The k_{cat} was calculated from V_{max}/[E], where [E] is the total enzyme concentration (determined using the Bradford method, *17*).

K_d Determinations. A FluoroMax-2 fluorometer (290 nm excitation) was used to monitor fluorescence quenching for 50 mM K^+Hepes/0.2 M KCl/1 mM DTT (pH 7.5, 25 °C) solutions containing wild-type or mutant 4-HBA-CoA thioesterase and varying concentrations of 4-HBA-CoA or 4-hydroxyphenacyl-CoA ligand. For a typical titration experiment, 1 μL aliquots of ligand were added to a 1 mL solution of 0.5 μM thioesterase, and the fluorescence intensity at 334 nm measured following each addition.

The fluorescence data, collected at ligand concentrations ranging from 0 to 12 μM, were fitted to eq 3 (*18*) using the Kaleida Graph computer program for nonlinear regression analysis:

$$\Delta F = (\Delta F_{max}[E])\{(K_d + [E] + [S]) - \sqrt{(K_d + [E] + [S])^2 - 4[E][S]}\}/2 \quad (3)$$

where [S] is the total ligand concentration, [E] is the total enzyme concentration, K_d is the apparent dissociation constant of the enzyme-ligand complex, ΔF is the observed change in fluorescence intensity, and ΔF_{max} is the maximum change in fluorescence intensity.

^{31}P NMR Spectra. Thioesterase was prepared as described in ref *14*, except that Butyl-Sepharose column chromatography was substituted for Hydroxyapatite column chromatography. The proton-decoupled ^{31}P NMR spectra were recorded at 202.5 MHz, pH 7.5, and 5 °C using 5 mm NMR tubes and a Bruker AC−F 500 NMR spectrometer (calibrated with 85% phosphoric acid) at 202.5 MHz.

Raman Spectra. The nonresonant Raman spectra were obtained using 647.1 nm laser excitation from Innova 400 krypton laser system (Coherent, Inc.), a back-illuminated charge-coupled devise (CCD) detector (Model 1024EHRB/1, Princeton Instruments, Inc.) operating at 183K, and a Holospec f/1.4 axial transmission spectrometer (Kaiser Optical Systems, Inc.) employed as a single monochromator, as described in a previous report (*19*). Enzyme samples, contained in cuvettes, were 50 μL in volume and buffered with 25 mM Tris-HCl at pH 7.5. Enzyme and 4-HBA-CoA or 4-hydroxyphenacyl-CoA concentrations used are given in the figure legends. Data were collected immediately after the complex had been made, using a laser power of ~900 mW and CCD exposure times of 5 min. The Raman spectrum of the buffer was subtracted from that of the ligand in buffer (giving the spectrum of free ligand), while the spectrum of the enzyme in buffer was subtracted from that of the enzyme-ligand complex to give the spectrum of the bound ligand. Wavenumber calibration yields Raman band positions to within ± 1 cm^{-1} for sharp bands.

RESULTS

Evaluation of CoA Binding. The structure of the D17N thioesterase-4-HBA-CoA complex shows the hydroxybenzoyl-pantetheine segment buried in a "worm hole" and the nucleotide segment resting on the protein surface (see two different perspectives of ligand bound to the thioesterase tetramer shown in Figure 2). The topology of the protein surface surrounding the active site entrance is striking in that it resembles a cupped hand, with positively charged fingers that surround the cradled nucleotide. The close proximity of the nucleotide phosphoryl groups to the positively charged surface residues (Arg126, Arg128, Arg88, Arg89, and Lys90) suggested that electrostatic forces may guide the substrate to the active site and then bind the nucleotide moiety to the protein surface.

Close inspection of the polar enzyme groups that are positioned for interaction with the substrate nucleotide moiety, however, gave an unexpected result: ion pair formation does not occur with any one of the five positively charged side chains. Instead, the 5′-αP-βP unit interacts with two water molecules (one of which binds to the ammonium group of Lys90), while the 3′-P is bound by the backbone amide NHs of Arg89, Lys90, and the side chain of Ser91 (see Figure 3). Additional binding interaction takes place between the Ade N(3) and a water molecule bound by the side chain of Arg88 and between the Ade C(6)NH_2 and N(8) and a water molecule bound to the backbone amide C═O of Phe68. One might question whether the mode of nucleotide binding observed in the crystal structure derive from crystal packing forces. In solution, the nucleotide segment may not bind the enzyme surface, or it may bind to the surface in an orientation that optimizes interaction between the positively charged residues and the negatively charged phosphates.

To determine whether the CoA nucleotide binds with the enzyme surface or simply "dangles" in solution, kinetic and spectral investigations were carried out.

Kinetic Evidence for a CoA Binding Site. First, CoA was tested as a competitive inhibitor of thioesterase catalyzed 4-HBA-CoA hydrolysis. The observed competitive inhibition, K_i = 370 μM, is evidence for a substrate CoA binding site. The next issue addressed was whether the nucleotide, or simply the pantetheine arm, is bound by the thioesterase. As is seen in the X-ray structure, the pantetheine arm is bound through NHs by the backbone C═Os of Ile61and Phe68, through the C═Os by two water molecules, and through the OH by the backbone NH of Ala129 (Figure 3). To determine the contribution of the nucleotide unit to productive substrate binding the truncated analogue, 4-hydroxybenzoyl-pantetheine (Chart 1), was tested as substrate. The result was k_{cat} = 0.74 s^{-1} and K_m = 270 μM (vs k_{cat} = 18 s^{-1} and K_m = 6 μM for 4-HBA-CoA). The 1000-fold decrease observed in k_{cat}/K_m showed that the nucleotide unit was indeed required for substrate recognition. This suggested that the nucleotide unit binds to a specific region on the enzyme. Nucleotide binding was tested using the ^{31}P NMR approach described below.

^{31}P NMR Evidence for a CoA 3′-P Binding Site. In the crystal, the CoA 3′-P forms several H-bonds to the thioesterase

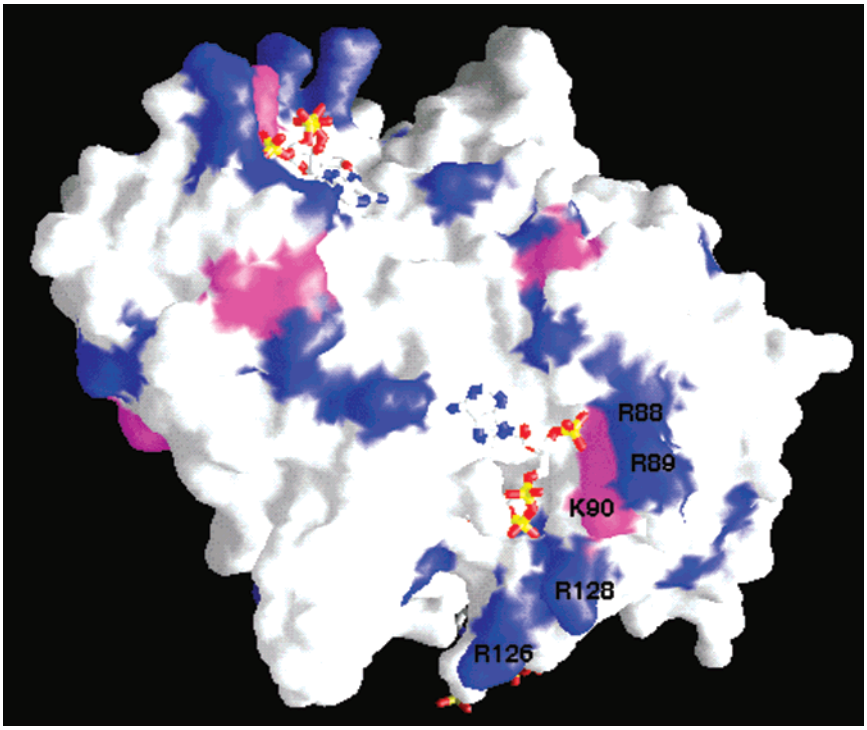

FIGURE 2: GRASP representation of the surface topology of the *Pseudomonas* sp. strain CBS3 4-HBA-CoA thioesterase D17N mutant tetramer (*13*) with stick-figure 4-HBA-CoA ligands. The Arg residues are blue and the Lys magenta.

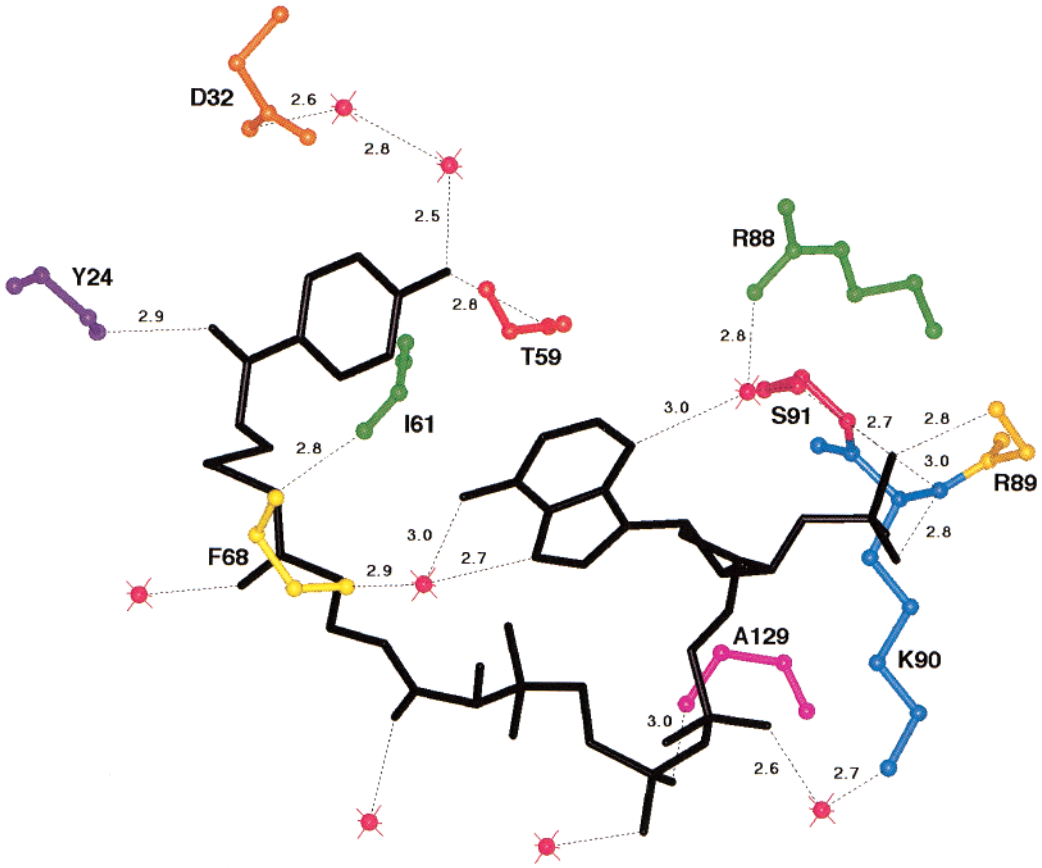

FIGURE 3: Diagram of the 4-HBA-CoA thioesterase residues within 3.5 Å of the 4-hydroxyphenacyl-CoA ligand generated using Insight II and the coordinates reported in ref *13*.

surface (Figure 3). If these interactions are preserved when the enzyme−ligand complex is in solution, the 3′-P would experience an electronic environment different from that of pure solvent. Thus, a difference in chemical shift of the 3′-P ^{31}P NMR resonance from solvated enzyme−ligand complex versus that of solvated unbound ligand would signify association of the 3′-P with the enzyme surface. The proton-decoupled ^{31}P NMR spectrum of 4-hydroxyphenacyl-CoA

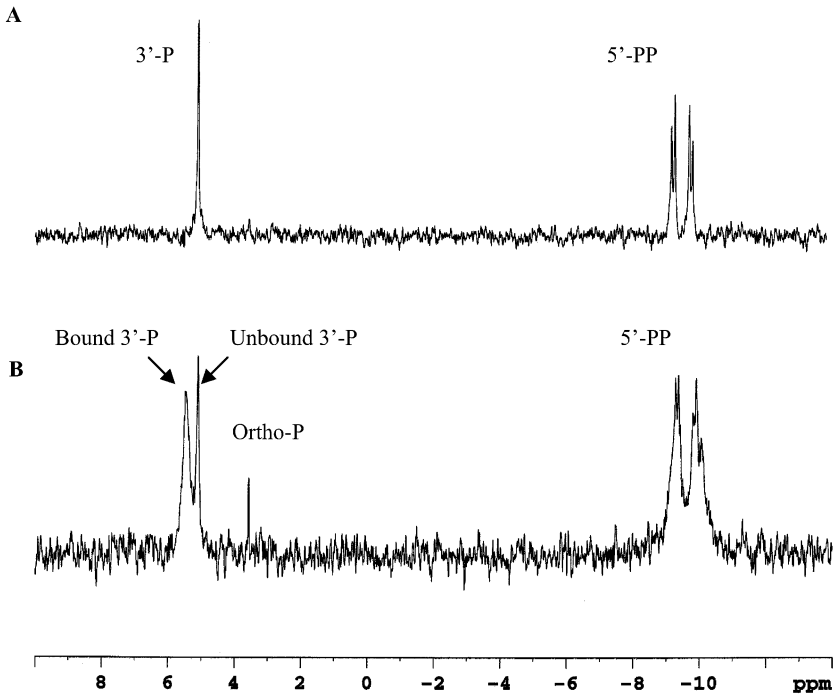

FIGURE 4: ^{31}P NMR spectrum of 1 mM 4-hydroxyphenacyl-CoA at pH 7.5 (A) and ^{31}P NMR spectrum of an equal molar mixture (1 mM each) of wild-type 4-HBA-CoA thioesterase and 4-hydroxyphenacyl-CoA at pH 7.5 with orthophosphate internal standard (3.5 ppm) (B).

in Hepes buffer was characterized by a singlet at + 5.05 ppm and two doublets (J = 20 Hz) centered at − 9.36 and −9.90 ppm, respectively (Figure 4). The singlet was assigned to the CoA 3′-P, while the two doublets were assigned to the 5′-PP. The ^{31}P NMR spectrum of bound 4-hydroxyphenacyl-CoA was characterized by a broad singlet at + 5.43 ppm, 0.38 ppm downfield from the singlet at + 5.05 ppm. The downfield singlet corresponded to the CoA 3′-P of the enzyme bound ligand while the singlet at + 5.05 ppm corresponded to the CoA 3′-P of the unbound ligand. (Because of faster relaxation in the latter, its signal is disproportional to its concentration.) The broadening of the signal (24.2 Hz at half-height vs 7.5 Hz for the unbound ligand) is caused by the slow tumbling rate of the tetrameric enzyme complexed with ligand (67.6 kDa) and the restricted motion in the 3′-P. The signals from the 5′-PP group are similarly broadened but not noticeably shifted. The absence of large perturbations in chemical shift is compatible with extensive hydration of the bound 3′-P and 5′-PP groups, as was suggested by the X-ray crystal structure.

Raman Evidence for an Adenine Binding Site. The Raman difference spectra measured for the wild-type thioesterase-4-hydroxyphenacyl-CoA and D17N thioesterase-4-HBA-CoA complexes (Figure 5) indicate that the adenine ring in the solution enzyme-ligand complexes is in a similar or identical environment as that indicated by the X-ray crystallographic results. The adenine ring displays a characteristic triplet pattern seen in the Figure 5A top spectrum at 1309, 1341, and 1380 cm^{-1} (the 1309 cm^{-1} peak is obscured in the Figure 5B top spectrum by modes from another part of the molecule). Upon binding, the triplet pattern is perturbed, but only slightly, indicating weak interactions between the ring and the protein. In the CoA binding enzymes where protein−adenine interactions occur in the absence of solvent, the triplet shows major changes, e.g., when a CoA-based substrate binds to 4-chlorobenzoyl CoA dehalogenase the bands move as follows (free to bound), 1379 to 1375, 1340 to 1329, and 1309 to 1302 cm^{-1} (shoulder) (*19*, 20).

Contribution of the 3′-P to Stabilization of the Enzyme−Substrate Complex. The multiple H-bonds formed with the 3′-P of the bound substrate (Figure 3) could serve as a major source of binding energy. However, because the H-bonds formed between the nucleotide 3′-P and the enzyme surface replace H-bonds to solvent molecules, their actual contribution to ligand binding energy might be small. The 4-HBA-(3′-dephospho)CoA analogue was used to measure this contribution. The k_{cat} = 19 s^{-1} of 4-HBA-(3′-dephospho)-CoA was essentially the same as that of the natural substrate, while the K_m = 19 ± 1 μM was increased 3-fold. For 4-HBA-CoA binding to D17N thioesterase, the K_d = 0.15 μM, and for 4-HBA-(3′-dephospho)CoA, the K_d is 0.44 μM. Thus, the contribution of the 3′-phosphate group to stabilization of the ES complex, 0.64 kcal/mol, is small but significant, consistent with the hydrated binding site suggested by the crystal structure.

Positively Charged Surface Residues at the CoA Binding Site. What role, if any, do the positively charged side chains of Arg126, Arg128, Arg88, Arg89, and Lys90 surrounding the nucleotide play in substrate binding? To address this question, each residue was replaced with Ala and/or Leu and the catalytic (k_{cat}, k_{cat}/K_m) and inhibitor (4-hydroxyphenacyl-CoA) binding properties of the mutants determined (see Table 1). For R88A, R89L, R126L, and R128A, no significant reductions in k_{cat}, k_{cat}/K_m, or 4-hydroxyphenacyl-CoA binding were found. For K90A the k_{cat} was unchanged, but the k_{cat}/K_m and 4-hydroxyphenacyl-CoA binding affinity were decreased slightly (2−3-fold).

Lys90 is the only positively charged residues whose side chain interacts with the substrate in the crystal structure. The interaction occurs with the β-phosphoryl group of the nucleotide pyrophosphate group via an intervening water molecule. Individually, the positively charged chains do not

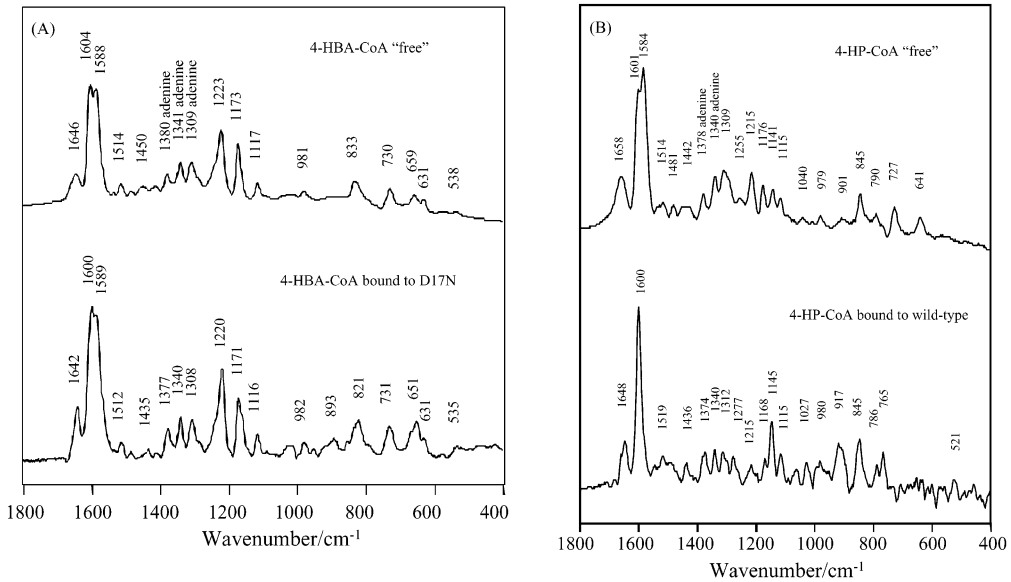

FIGURE 5: (A) Raman difference spectra of 5 mM 4-HBA-CoA in 25 mM Tris, 0.5 M KCl, pH 7.5 (top), and of a D17N thioesterase 4-HBA-CoA complex (1.2 mM enzyme, 0.8 mM 4-HBA-CoA, 25 mM Tris, 0.5 M KCl, pH 7.5 (bottom). (B) Raman difference spectra of 1.08 mM 4-hydroxyphenacyl-CoA (4-HP-CoA) in 25 mM Tris, 0.15 M KCl, pH 7.5 (top), and of a wild-type thioesterase−4-hydroxyphenacyl-CoA complex (1.0 mM enzyme, 320 μM 4-HP-CoA, 25 mM Tris, 0.15 M KCl, pH 7.5) (bottom).

Table 1: Steady-State Kinetic Constants Determined for Wild-Type and Mutant 4-HBA-CoA Thioesterase with 4-HBA-CoA Serving as Substrate at pH 7.5 and 25 °C[a]

	4-HBA-CoA		4-HP−CoA	
thioesterase	k_{cat} (s^{-1})	K_m (μM)	K_d (μM)	K_i (μM)
wild-type	1.8×10^1	6.0	3.4×10^{-1}	1.4
D17E	4.8×10^{-1}	2.4	ND	1.8
D17N	5.5×10^{-4}	1.5×10^{-1}(K_d)	4.2×10^{-1}	ND
D17S	8.4×10^{-4}	ND	ND	ND
R88A	1.3×10^1	4.5	9.4×10^{-1}	1.2
R89L	1.8×10^1	5.2	1.3	ND
K90A	1.4×10^1	1.4×10^1	ND	4.0
R126L	1.1×10^1	5.0	ND	1.1
R128A	1.5×10^1	7.3	ND	2.1

[a] Also listed are competitive inhibition constants (K_i) and dissociation constants (K_d) (determined using fluorescence quenching methods) measured for 4-HBA-CoA or 4-hydroxyphenacyl-CoA (4-HP−CoA). See Materials and Methods Section for details. The reported values are defined within 10% error. ND is an abbreviation for "not determined".

make a substantial contribution to substrate binding and catalysis.

Catalytic Role of Asp17. Figure 6 shows the arrangement of groups in the thioesterase catalytic site. Asp17 is the only polar residue in close vicinity of the thioester C═O. To evaluate the contribution made by the Asp17 to catalysis, site-directed mutants were prepared and analyzed. The substrate k_{cat} and K_m values and the 4-hydroxyphenacyl-CoA dissociation (K_d) or inhibition (K_i) constants determined for the D17E and D17N mutants are listed Table 1. Comparable substrate K_m and 4-hydroxyphenacyl-CoA K_i values for the wild-type and D17E thioesterases showed that the replacement of Asp17 with Glu has little impact on substrate binding. On the other hand, the k_{cat} was reduced 38-fold. Because of the longer side chain of the Glu residue ($CH_2CH_2COO^-$ vs CH_2COO^-), the positioning of the carboxylate group in the mutant may not be optimized for catalysis.

Substitution of the carboxylate group with an amide, as in the D17N mutant, had a pronounced effect on catalysis (k_{cat} is reduced 3×10^4-fold) but no effect on substrate binding (based on 4-hydroxyphenacyl-CoA K_d). Because the active site conformation is unaltered in this mutant, we can attribute the loss of activity to the inability of the Asn amide to function in place of the carboxylate group. The D17S mutant, in which a CH_2OH substitutes for the COO^- group, was also strongly inhibited (2×10^4-fold reduction in k_{cat}). Thus, the hydroxyl group is also unable to perform the catalytic role of the carboxylate group.

Carbonyl Polarization. The substrate thioester C═O is positioned to interact with the positive pole of the active site α-helix macrodipole and to H-bond with the backbone amide NH of Tyr24 (the helix N-terminal residue) (see Figure 6). Raman spectroscopy was used to measure the extent to which these interactions polarize the thioester C═O. 4-HBA-CoA in buffer (pH 7.5) gives rise to a carbonyl stretching vibration of the thioester at 1646 cm^{-1}, phenyl ring C═C stretching modes (8a and 8b) at 1604 and 1588 cm^{-1}, and in-plane phenyl hydrogen bending modes at 1223 and 1173 cm^{-1} (*19*, *20*). The Raman difference spectra of 4-HBA-CoA in buffer (25 mM Tris pH 7.5 and 0.5 M KCl) and bound to the D17N thioesterase are shown in Figure 5A. The bandwidth of the thioester C═O stretching mode of solvated 4-HBA-CoA at 1646 cm^{-1} is broad (35 cm^{-1} at half-height) compared to the feature seen at 1642 cm^{-1} that derives from the thioester C═O of enzyme bound 4-HBA-CoA (22 cm^{-1} at half-height), indicating that the ligand C═O is conformationally restricted by the thioesterase active site. The C═O group is in a more uniform environment in the active site than when free in aqueous solution. In solution, the C═O band is broadened by a rapidly changing heterogeneous environment caused by the motion of the water molecules. Another possible source of broadening is torsional motions about the Ph−C(═O)−S bonds, these may become more restricted in the active site, leading to a narrow C═O profile. The small frequency shift (from 1646 to 1642 cm^{-1})

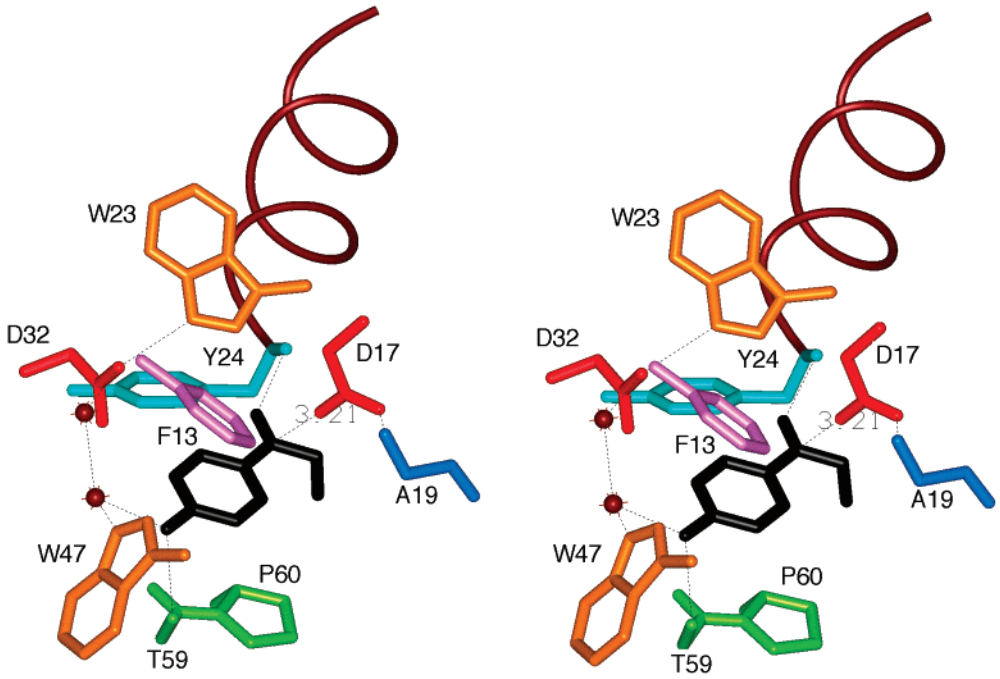

FIGURE 6: Stereodiagram of the catalytic site of the wild-type 4-HBA-CoA thioesterase with 4-hydroxyphenacyl-CoA truncate bound (black) generated using Insight II and the coordinates reported in ref *13*.

indicates that the H-bonding to the 4-HBA-CoA thioester C═O may be only slightly greater in the thioesterase active site than it is in buffer. The C(═O)—S stretching contributes to the 833 cm^{-1} band observed in the spectrum of solvated 4-HBA-CoA (*19*). This feature is downshifted to 821 cm^{-1} in the spectrum of the thioesterase-bound substrate, indicating a decrease in the scissile C—S bond order. The S—C stretching band in the pantetheine unit is shifted slightly from 659 to 651 cm^{-1}. The phenyl ring C═C stretching modes observed for solvated 4-HBA-CoA at 1604 and 1588 cm^{-1} are shifted only slightly to 1600 and 1589 cm^{-1} when the 4-HBA-CoA binds to the active site. The other ring modes at 1223 and 1173 cm^{-1} are shifted only slightly to 1220 and 1171 cm^{-1}.

The π-electron density of the benzoyl ring of 4-HBA-CoA does not appear to be strongly polarized by the active site of D17N thioesterase. Indeed, the phenol and not the quinone methide form of the 4-HBA-CoA is the major contributor to the spectrum. The C═O stretching shifts from 1663 cm^{-1} (in CCl_4) to 1642 cm^{-1} in the D17N thioesterase active site. This shift corresponds an enthalpy of H-bonding of 4.3 kcal/mol (*21*), equivalent to about one mid-strength H-bond, which is consistent with what was seen in the X-ray structure of the D17N thioesterase-4-HBA-CoA complex (Figure 6).

By using the 4-hydroxyphenacyl-CoA ligand in place of 4-HBA-CoA, we were able to probe the environment of the active site of the wild-type thioesterase. The Raman difference spectra of 4-hydroxyphenacyl-CoA in buffer (25 mM Tris pH 7.5 and 0.15 M KCl) and bound to the wild-type thioesterase are shown in Figure 5B. The bandwidth of the ketone C═O stretching mode of solvated 4-hydroxyphenacyl-CoA at 1658 cm^{-1} is broad (44 cm^{-1} at half-height) compared to the feature seen at 1648 cm^{-1} that derives from the ketone C═O of enzyme-bound 4-hydroxyphenacyl-CoA (30 cm^{-1} width), indicating that the ligand C═O is in a more uniform environment in the thioesterase active site compared to what it experiences in solution. Again, the small frequency shift (from 1658 to 1648 cm^{-1}) indicates that the H-bonding to the 4-hydroxyphenacyl-CoA ketone C═O may be only slightly greater in the thioesterase active site than it is in buffer. The phenyl ring C═C bands of the ligand in buffer occur at 1601 and 1584 cm^{-1}. These features appear to merge into a single band at 1600 cm^{-1} observed in the spectrum of the thioesterase bound 4-hydroxyphenacyl-CoA. Overall, these changes are modest.

DISCUSSION

This study examined three aspects of 4-HBA-CoA thioesterase catalysis: (1) binding of the CoA nucleotide, (2) the contribution of Asp17, and (3) the polarization of the substrate thioester C═O.

The polarization of the substrate C═O was examined using Raman spectroscopy.

The 4-HBA-CoA benzoyl and C═O Raman signals can be easily discerned in the Raman difference spectra. Previous studies have shown that an enzyme active site which induces the movement of electron density from the 4-HBA-CoA hydroxybenzoyl ring onto the thioester oxygen causes a dramatic alteration in the H—C═C and C═O Raman modes (*19*—*21*). Such a dramatic change did not occur with the 4-HBA-CoA bound to the thioesterase. Instead, a significant decrease in bandwidth accompanied a modest shift in the carbonyl stretch mode upon transfer of the 4-HBA-CoA from water to the active site environment. These changes are indicative of a decrease in C═O conformational freedom and a slight increase in C═O polarization resulting from interaction with the backbone amide NH of Tyr24, the N-terminal residue of the active site α-helix (Figure 6). C═O immobilization as well as polarization may facilitate the attack of the nucleophile at the carbonyl carbon (*22*).

The participation of Asp17 in thioesterase catalysis was suggested by the close proximity of its carboxylate group to the substrate thioester C═O. The substitution of Asp17 with

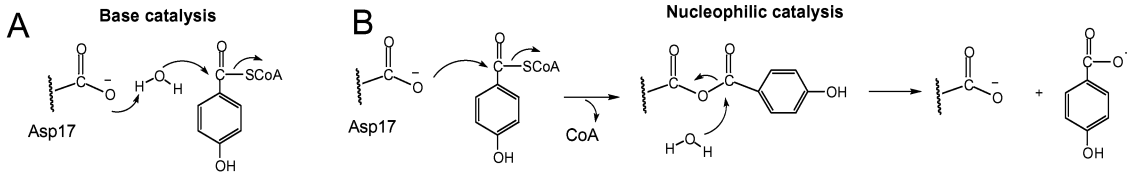

FIGURE 7: Mechanisms for thioesterase catalysis with Asp17 serving in the role of (A) general base or (B) nucleophile.

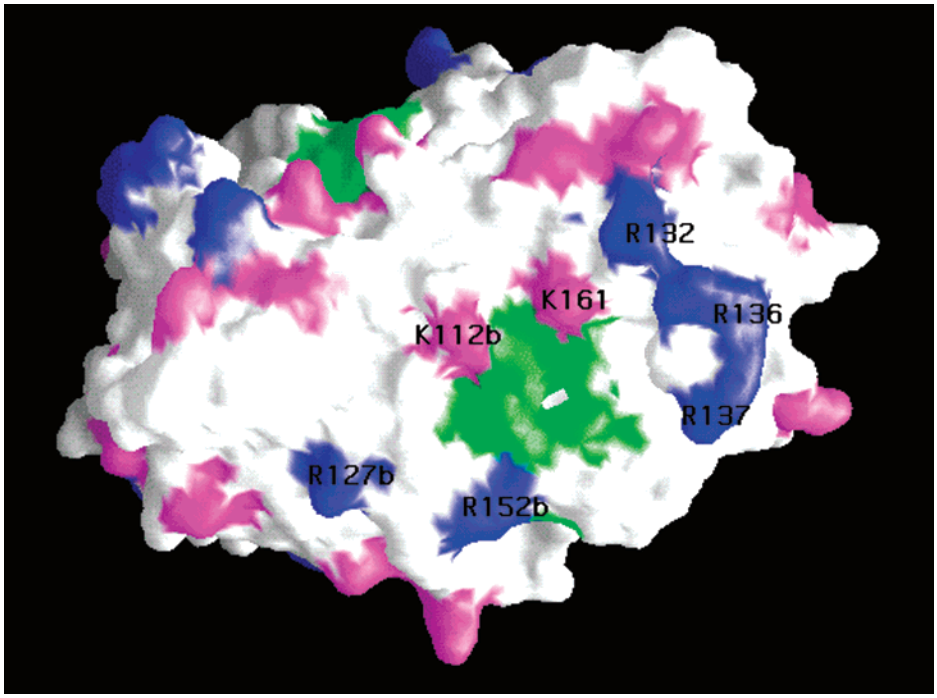

FIGURE 8: GRASP representation of the surface topology of *E. coli* β-hydroxydecanoyl-ACP desaturase dimer (*11*). The location of the active site entrance is shown in green and the positively charged residues in blue and purple.

Glu resulted in a moderate (38-fold) reduction in catalysis, while the substitution with Asn or Ser resulted in a dramatic reduction (10^4-fold) in catalysis. The catalytic role played by Asp17 has yet to be determined. One possibility is general base catalysis (see Figure 7A). However, one would anticipate a water bound between the carboxylate and the C═O in the crystal structure or at least, the proper distancing between the carboxylate and the carbonyl to allow a water molecule to bind. Instead, the Asp17 carboxylate is positioned within 3.2 Å of the C═O and aligned (96° trajectory) for nucleophilic attack (Figure 6). This arrangement is highly suggestive of nucleophilic catalysis, proceeding via an aspartyl-4-hydroxybenzoyl anhydride intermediate (Figure 7B). Precedent for formation of an anhydride intermediate is found in the phosphotransferases of the HAD enzyme family which are known to form aspartyl phosphate intermediates (*23*−*28*), in the transferases succinyl-CoA:3-ketoacid CoA-transferase (*29*−*30*) and glutaconate CoA-transferase (*31*−*32*), which form carbon anhydride intermediates (using an active site Glu as the acyl acceptor). Studies aimed at distinguishing between the two reaction pathways shown in Figure 7 are in progress.

The X-ray crystal structure of liganded enzyme coupled with results from the ^{31}P-NMR and substrate analogue studies suggest that the substrate nucleotide moiety is anchored to the protein surface. While single replacements made among the positively charged residues at the nucleotide binding site had little impact on catalysis, we cannot dismiss the possibility that collectively these charges guide nucleotide and, hence, substrate binding.

Although the nucleotide sits outside of the active site crevice, it is surrounded by surface projections, which are complementary, in shape and charge, to the nucleotide. The nucleotide rests in a snug, albeit watery, cradle. Members of the hotdog-fold family that catalyze reactions of acyl-CoA substrates are likely to conserve this site while members which catalyze reactions of acyl-ACP substrates, wherein the pantetheine arm attaches to a carrier protein rather than a nucleotide, are not. Indeed, the GRASP representation of the *E. coli* β-hydroxydecanoyl-ACP desaturase (*11*) shown in Figure 8 reveals a convex protein surface encircling the active site, not at all similar to the region surrounding the active site in the 4-HBA-CoA thioesterase. Located near the active site of the desaturase (indicated in green) is a patch of positively charged residues (blue and magenta) that bind to a patch of negatively charged residues at the pantetheine attachment site on the docked acyl carrier protein (*11*). Thus, the charge and topology of the surface region surrounding the active site of a hotdog-fold enzyme may allow a distinction to be made between activity directed at an acyl-CoA substrate versus an acyl-ACP substrate, based on structural data alone.

REFERENCES

1. Benning, M. M., Wesenberg, G., Liu, R., Taylor, K. L., Dunaway-Mariano, D., and Holden, H. M. (1998) *J. Biol. Chem. 273*, 33572−33579.

2. Li, J., Derewenda, U., Dauter, Z., Smith, S., and Derewenda, Z. S. (2000) *Nature Struct. Biol. 7*, 555−559.
3. Tsai, S.-C., Miercke, L. J. W., Krucinski, J., Gokhale, J. C.-H., Chen, P. G., Foster, P. G., Cane, D. E., Khosla, C., and Stroud, R. M. (2001) *PNAS 98*, 14808.
4. Bruner, S. D., Weber, T., Kohli, R. M., Schwarzer, D., Maraheil, M. A., Walsh, C. T., and Stubbs, M. T. (2002) *Structure 10*, 301.
5. Devedjiev, Y., Dauter, Z., kuznetsov, S., Jones, T., and Derewenda, Z. *Structure 8*, 1137 (2000).
6. Bellizzi, J. J. III, Widom, J., Kemp, C., Lu, J. Y., Das, A. K., Hofmann, S. L., and Clardy, J. (2000) *PNAS 97*, 4573.
7. Lawson, D. M., Derewenda, U., Serre, L., Ferri, S., Szitter, R., Wei, Y., Meighen, E. A., and Derewenda, Z. S. (1994) *Biochemistry 33*, 9382.
8. Hunt, M. C., and Alexson, S. E. H. (2002) *Prog. Lipid Res. 41*, 99.
9. Heathcote, M. L., Staunton, J., and Leadlay, P. F. (2001) *Chem. Biol. 8*, 207.
10. Duncan, J. A., and Gilman, A. G. (1998) *J. Biol. Chem. 273*, 15830.
11. Leesong, M., Henderson, B. S., Gillig, J. R., Schwab, J. M., and Smith J. L. (1996) *Structure 4*, 253−264.
12. Dunaway-Mariano, D., and Babbitt, P. C. (1994) *Biodegradation 5*, 259−276
13. Thoden, J. B., Holden, H. M, Zhuang, Z. and Dunaway-Mariano, D. (2002) *J. Biol. Chem.* (in press).
14. Chang, K.-H., Liang, P.-H., Beck, W., Scholten, J. D., and Dunaway-Mariano, D. (1992) *Biochemistry 31*, 5606−5610.
15. Luo, L., Taylor, K. L., Xiang, H., Wei, Y., Zhang, W., Dunaway-Mariano, D. (2001) *Biochemistry 40*, 15684−92.
16. Erlich, H. A. (1992) *PCR Technology Principles and Applications for DNA Amplification*, W. H. Freeman and Co., New York.
17. Bradford, M. M. (1976) *Anal. Biochem. 72*, 248−254.
18. Anderson, K. S., Sikorski, J. A., and Johnson, K. A. (1988) *Biochemistry 27*, 1604−1610.
19. Dong, J., Xiang, H., Luo, L., Dunaway-Mariano, D., and Carey, P. R. (1999) *Biochemistry 38*, 4198−4206.
20. Taylor, K. L., Liu, R. Q., Liang, P. H., Price, J., Dunaway-Mariano, D., Tonge, P. J., Clarkson, J., and Carey, P. R. (1995) *Biochemistry 34*, 13881−13888.
21. Clarkson, J., Tonge, P. J., Taylor, K. L., Dunaway-Mariano, D., and Carey, P. R. (1997) *Biochemistry 36*, 10192−10199.
22. Lightstone, F. C., and Bruice, T. C. (1996) *J. Am. Chem. Soc. 118*, 2595−2605.
23. Cantley, L. C., Jr., Cantley, L. G., and Josephson, L. (1978) *J. Biol. Chem. 253*, 7361−7368.
24. Missiaen, L., Wuytack, F., De Smedt, H., Vrolix, M., and Casteels, R. (1988) *Biochem. J. 253*, 827−833.
25. Murphy, A. J., and Coll, R. J. (1993) *J. Biol. Chem. 268*, 23307−23310.
26. Pick, U. (1982) *J. Biol. Chem. 257*, 6111−6119.
27. Troullier, A., Girardet, J. L., and Dupont, Y. (1992) *J. Biol. Chem. 267*, 22821−22829.
28. Solomon, F., and Jencks, W. P. (1969) *J. Biol. Chem. 244*, 1079−1081.
29. Rochet, J.-C., and Bridger, W. A. (1994) *Protein Sci. 3*, 975−981.
30. Mack M., and Buckel, W. (1997) *FEBS Lett. 405*, 209−212.
31. Jacob, U., Mack, M., Clausen, T., Huber, R., Buckel, W., and Messerschmidt, A. (1997) *Structure 5*, 415−426.
32. Kraulis, P. J. (1991) *J. Appl. Crystallogr. 24*, 946−950.

BI0262303